

Protocol for scaling up a sign-ordered Kitaev chain without magnetic flux control

Chun-Xiao Liu,^{1,*} Sebastian Miles,¹ Alberto Bordin,¹ Sebastiaan
L. D. ten Haaf,¹ A. Mert Bozkurt,¹ and Michael Wimmer¹

¹*QuTech and Kavli Institute of Nanoscience, Delft University of Technology, Delft 2600 GA, The Netherlands*
(Dated: July 8, 2024)

Quantum dot-superconductor arrays have emerged as a new and promising material platform for realizing Kitaev chains with Majorana zero modes. So far, experiments have implemented a two-site chain with limited protection. We propose a protocol for scaling up the Kitaev chain that is accessible to current experiments and optimizes the Majorana protection. To this end, we make use of the fact that the relative sign of normal and superconducting hoppings mediated by an Andreev bound state can be changed by electrostatic gates. In this way, our method only relies on the use of individual electrostatic gates on hybrid regions, quantum dots, and tunnel barriers, respectively, without the need for individual magnetic flux control, greatly simplifying the device design. Our work provides guidance for realizing a topologically protected Kitaev chain, which is the building block of error-resilient topological quantum computation.

Introduction.—The Kitaev chain is a one-dimensional model of spinless fermions with p -wave superconducting pairing [1]. It is a paradigm of topological superconductivity which can host localized Majorana zero modes at the endpoints [2–15]. These exotic mid-gap excitations, characterized by their non-Abelian statistics, are regarded as the building blocks for the implementation of error-resilient topological quantum computation [16, 17].

Recently, quantum dot-superconductor arrays have emerged as a promising platform for realizing a Kitaev chain, where spin-polarized dot orbitals form spinless fermions [18]. A minimal two-site version [19] has been successfully realized in both nanowires and two-dimensional electron gases, supported by tunnel spectroscopic evidence of Majorana zero modes at a sweet spot [20–22]. Crucially, a balance of the normal and superconducting coupling strengths, which are now mediated by Andreev bound states, is achieved by changing the chemical potential in the superconducting region [23–26]. However, these finely-tuned zero modes remain vulnerable to environmental noise, since the protection against on-site energy fluctuations is only quadratic and there is no protection against coupling fluctuations [19, 23, 27–33]. To obtain topological protection, the quantum dot array has to be scaled up [34, 35] such that the chain length is much larger than the Majorana localization length [1, 18, 36].

In contrast to the two-site version, in an extended Kitaev chain ($N \geq 3$), the phases of the couplings become particularly important for obtaining protected Majorana zero modes. In the limit of confinement to a one-dimensional channel as in experiments [20–22] and in the presence of Rashba spin-orbit interaction and an axial magnetic field, it has been pointed out that an approximate complex conjugate symmetry [37] further constrains the effective couplings to be real numbers [18]. In particular, this symmetry is expected when the spin-orbit

length l_{SO} is larger than the width W of the channel, $l_{\text{SO}} > W$ [38, 39]. Thus, the problem of phase uncertainty is now reduced to *sign* uncertainty. Under these assumptions, for an N -site Kitaev chain

$$H_K = \sum_{n=1}^N \varepsilon_n f_n^\dagger f_n + \sum_{n=1}^{N-1} (t_n f_{n+1}^\dagger f_n + \Delta_n f_{n+1}^\dagger f_n^\dagger + h.c.), \quad (1)$$

the condition for obtaining optimally protected Majorana zero modes becomes

$$\varepsilon_n = 0, \quad |t_n| = |\Delta_n|, \quad \text{sgn}(t_1 \Delta_1) = \text{sgn}(t_n \Delta_n). \quad (2)$$

Here N is the total number of sites, f_n is the annihilation operator of the n -th fermion, ε_n is the onsite energy, and t_n and Δ_n are the amplitudes of normal and superconducting tunnelings, respectively. Note that the problem of sign uncertainty was first discussed in Ref. [18], where it was proposed to obtain a sign-ordered chain by individual control of the superconducting phase in each superconducting grain. This requires the introduction of multiple flux bias lines, which would inevitably increase the device size and complicate the device design [see Fig. 1(a)].

In the current work, we propose a scale-up protocol for the Kitaev chain, where the sign problem is fixed purely in an electrostatic way without magnetic flux control [see Fig. 1(b)]. We find that the two sweet spots mediated by an Andreev bound state have opposite signs, which was overlooked and undetectable in the previous studies of two-site chains [20–23, 27–29, 40–42]. This subtle sign difference can be explicitly detected in a three-site setup by conductance spectroscopy. Based on this, we give our protocol for scaling up, emphasizing how to choose a correct sweet spot in each pair of double quantum dots by varying the electrostatic gates nearby. Since our method does not rely on magnetic flux control, it greatly simplifies the device design and makes the platform suitable for implementing scalable topological quantum computation.

* Corresponding author: chunxiaoliu62@gmail.com

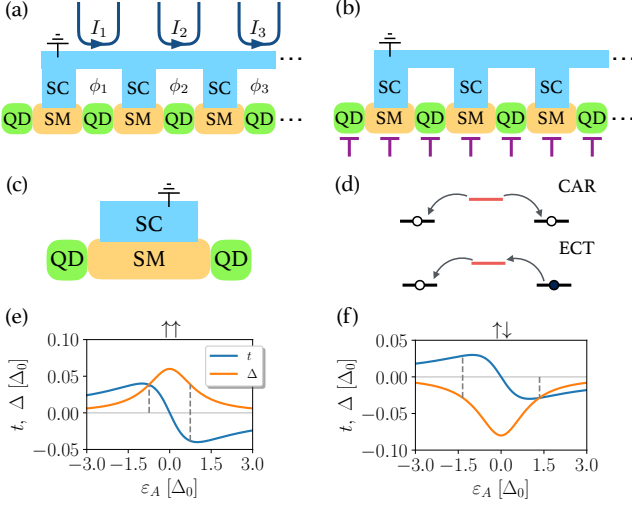


FIG. 1. (a) Schematic of a device with magnetic flux control. The flux bias lines control the phase difference in each individual superconducting loop. (b) Schematic of the device considered in this work, where the signs of the effective couplings are controlled completely by the voltages of the electrostatic gates near the quantum dots and the hybrid regions. (c) Schematic of a basic two-site Kitaev chain. (d) Schematic of the virtual processes that induce CAR and ECT couplings. (e) and (f) Dependence of CAR (Δ) and ECT (t) amplitudes on the chemical potential of the Andreev bound states.

Sign of sweet spot.—We first consider a minimal setup consisting of double quantum dots connected by a hybrid segment. The Hamiltonian is [23, 24, 27, 28, 43]

$$\begin{aligned}
 H &= H_{D,1} + H_{A,1} + H_{D,2} + H_{DAD,1}, \\
 H_{D,i} &= \sum_{\sigma=\uparrow,\downarrow} (\varepsilon_D i + \sigma E_{Zi}) n_{Di\sigma} + U_D i n_{Di\uparrow} n_{Di\downarrow}, \\
 H_{A,i} &= \sum_{\sigma=\uparrow,\downarrow} \varepsilon_{Ai} n_{Ai\sigma} + (\Delta_i c_{Ai\uparrow}^\dagger c_{Ai\downarrow} + h.c.), \\
 H_{DAD,i} &= \sum_{\sigma=\uparrow,\downarrow} \left(t_{sc,i} c_{Ai\sigma}^\dagger c_{Di\sigma} + t'_{sc,i} c_{Di+1\sigma}^\dagger c_{Ai\sigma} \right. \\
 &\quad \left. + \sigma t_{sf,i} c_{Ai\sigma}^\dagger c_{Di\sigma} + \sigma t'_{sf,i} c_{Di+1\sigma}^\dagger c_{Ai\sigma} + h.c. \right). \quad (3)
 \end{aligned}$$

Here H_D is the Hamiltonian for a quantum dot with a single spinful orbital, ε_D is the orbital energy, E_Z is the induced Zeeman spin splitting, and U_D is the strength of the on-site Coulomb repulsion. H_A is the Hamiltonian of subgap Andreev bound states (ABS) in the hybrid region, ε_A is the normal-state energy and Δ is the induced superconducting pairing. H_{DAD} describes single electron tunneling between dots and hybrids, t_{sc} is the amplitude for spin-conserving processes, while t_{sf} is for spin-flipping ones which is proportional to the strength of spin-orbit interaction in the system. Here we focus on the regime where the direction of the spin-orbit field and that of the applied magnetic field are perpendicular to each other [25, 26], making t_{sc}, t_{sf} real numbers [18, 37].

Note that the signs of t_{sc}, t_{sf} depend on microscopic details of the quantum dots, such as spin-orbit strength or dot orbitals.

In the tunneling regime where $|t_{sc}|, |t_{sf}| \ll \Delta, E_Z$, the effective couplings of quantum dots can be obtained using second-order perturbation theory as

$$\begin{aligned}
 t_{\uparrow\uparrow} &= (t_{sf,1} t'_{sf,1} - t_{sc,1} t'_{sc,1}) \frac{u^2 - v^2}{E_A}, \\
 \Delta_{\uparrow\uparrow} &= (t_{sc,1} t'_{sf,1} + t_{sf,1} t'_{sc,1}) \frac{2uv}{E_A}, \quad (4)
 \end{aligned}$$

where $t_{\uparrow\uparrow}$ and $\Delta_{\uparrow\uparrow}$ are the amplitudes of elastic co-tunneling (ECT) and crossed Andreev reflection (CAR) between spin-up orbitals in the quantum dots. $u^2 = 1 - v^2 = 1/2 + \varepsilon_A/2E_A$ are the coherence factors, and $E_A = \sqrt{\varepsilon_A^2 + |\Delta_0|^2}$ is the excitation energy of the ABS. Figure 1(e) shows the dependence of the two amplitudes on the chemical potential of the hybrid region, with model parameters $\Delta_1 = \Delta_0$, $t_{1sc} = t'_{1sc} = 0.3\Delta_0$ and $t_{1sf} = t'_{1sf} = 0.1\Delta_0$. We note that both amplitudes are real due to complex conjugate symmetry in the system [37]. Furthermore, the two sweet spots have opposite signs (indicated by dashed lines), i.e.,

$$\begin{aligned}
 t_{\uparrow\uparrow} &= \Delta_{\uparrow\uparrow}, \text{ for } \varepsilon_A = -\varepsilon_A^*, \\
 t_{\uparrow\uparrow} &= -\Delta_{\uparrow\uparrow}, \text{ for } \varepsilon_A = \varepsilon_A^*, \quad (5)
 \end{aligned}$$

where $\varepsilon_A^* = \Delta_0(t_{sc,1} t'_{sf,1} + t_{sf,1} t'_{sc,1}) / (t_{sf,1} t'_{sf,1} - t_{sc,1} t'_{sc,1}) = 0.75\Delta_0$ for our chosen parameter values. We emphasize that the existence of two opposite-sign sweet spots between CAR and ECT curves is a robust feature as evidenced by the form of Eq. (4). For example, when the strength of spin-orbit interaction becomes much stronger ($3t_{sc} = t_{sf} = 0.3\Delta_0$), the only effect is that $t_{\uparrow\uparrow}$ obtains an overall minus sign, while $\Delta_{\uparrow\uparrow}$ unchanged, thus only reversing the signs of the sweet spots relative to the weak spin-orbit-interaction scenario shown in Fig. 1(e). In addition, parity of the bound-state wavefunctions does not change the properties of the sweet spots either, because $t \rightarrow -t$ or $t' \rightarrow -t'$ would only give a common minus sign to both $t_{\uparrow\uparrow}$ and $\Delta_{\uparrow\uparrow}$. On the other hand, the coupling amplitudes between dot orbitals of opposite spin polarizations are

$$\begin{aligned}
 t_{\uparrow\downarrow} &= -(t_{sc,1} t'_{sf,1} + t_{sf,1} t'_{sc,1}) \frac{u^2 - v^2}{E_A}, \\
 \Delta_{\uparrow\downarrow} &= (t_{sf,1} t'_{sf,1} - t_{sc,1} t'_{sc,1}) \frac{2uv}{E_A}. \quad (6)
 \end{aligned}$$

Figure 1(f) shows the ε_A dependence of the two amplitudes using the same model parameters as those in Fig. 1(e). Now two sweet spots appear at $\varepsilon_A = \pm\varepsilon_A^*$ with $\varepsilon_A^* = \Delta_0(t_{sf,1} t'_{sf,1} - t_{sc,1} t'_{sc,1}) / (t_{sc,1} t'_{sf,1} + t_{sf,1} t'_{sc,1}) = 4\Delta_0/3$, and their signs are reversed relative to the same-spin scenario, i.e., now a negative (positive) ε_A corresponds to a same-(opposite-) sign sweet spot.

The position of the sweet spots in the model Hamiltonian (3) is symmetric around ε_A as we have assumed no

Zeeman splitting in the proximitized dot. In general, Zeeman splitting is expected to be reduced in a proximitized semiconductor [44, 45]. Nevertheless, it is still possible to find two sweet spots for a wide range of Zeeman splitting in the proximitized region [23], and continuity guarantees that the different sweet spots have opposite relative sign of t and Δ [46]. Hence, generically the relative sign of the effective normal and superconducting hopping between the normal quantum dots can be changed by either changing the energy of the Andreev bound state to switch to the other sweet spot, or by changing the dot energy to switch the spin occupation, i.e. using electrostatic gating.

Detection of π -phase shift.—To experimentally detect the subtle sign of sweet spots, the minimal setup to consider is a three-quantum-dot device with a superconducting loop connecting the two hybrid regions [see schematic in Fig. 2(a)]. When the sweet spots mediated by the two hybrid regions are of the same sign and dots are on resonance, the system would behave as a sign-ordered three-site Kitaev chain. By contrast, when the signs are opposite, it corresponds to a Kitaev chain with a π -phase domain wall. Moreover, tunnel conductance spectroscopy as a function of magnetic flux threading through the superconducting loop would distinguish between the two scenarios by a π -phase shift.

To support the above statements with numerical calculations, we consider the following Hamiltonian for the setup

$$H = H_{D1} + H_{A1} + H_{D2} + H_{A2} + H_{D3} + H_{DAD,1} + H_{DAD,2} \quad (7)$$

which includes three normal quantum dots connected by two Andreev bound states. The Hamiltonians for dots, ABSs and electron tunneling are almost identical to those in Eq. (3), except that now for H_A a phase difference determined by the magnetic flux is included in the pairing potential, i.e., $\Delta_1 = \Delta_0$, $\Delta_2 = \Delta_0 e^{i\Phi}$. In addition, a normal-metal lead is tunnel coupled to dot $D3$, and differential conductance is numerically calculated using the rate-equation method [47, 48]. The Hamiltonian parameters we choose for numerical calculations are (in unit of the induced gap $\Delta_0 = 1$): $|\Delta_i| = 1$, $3t_{sf,i} = t_{sc,i} = 0.3$, $E_{Zi} = 2$, $U_{Di} = 5$, dot-lead coupling strength $\Gamma = 0.005$, and electron temperature $k_B T = 0.005$, corresponding to the experimental devices recently studied in Refs. [20–22, 24–26, 34, 35].

We first consider a scenario where the sweet spots obtained in the two hybrid regions are of the same type. Assuming that all three quantum dots are spin-up and on resonance, this condition is satisfied when choosing $\varepsilon_{A1} = \varepsilon_{A2} \approx -0.804\Delta_0$, which is close to the values predicted by perturbation theory in Eq. (5). Figure 2(b) shows the conductance spectroscopy calculated at this point. Indeed, it indicates that a sign-ordered three-site Kitaev chain is obtained at $\Phi = 0$ with a stable and isolated zero-bias conductance peak being induced by Majorana zero modes, which is further protected by a finite

excitation gap. Additionally, this zero-bias peak is robust against detuning of dot $D3$, as shown in Fig. 2(c).

On the other hand, when we choose $\varepsilon_{A2} \approx 0.704\Delta_0$ while $\varepsilon_{A1} \approx -0.804\Delta_0$ still unchanged, the sign of the sweet spot mediated by $A2$ becomes opposite to $A1$ [see Fig. 1(e)], leading to the formation of a π -phase domain wall. As a result, as shown in Fig. 2(e), an additional zero-energy state appears in the vicinity of $\Phi = 0$, making the system gapless. Unlike the sign-ordered chain, now the zero-bias conductance peak is readily split with detuning of $D3$ [see Fig. 2(f)], owing to the hybridization between Majorana zero modes and the trivial zero-energy state induced by the domain wall. The splitting is $\delta E \approx t_1 \delta \varepsilon_3 / \sqrt{t_1^2 + t_2^2}$ with $t_{1,2}$ being the effective couplings defined in a spinless model Eq. (1) [46]. Moreover, by comparing Figs. 2(b) and 2(e) the sign switch of sweet spot is revealed as a π -phase shift in the flux-dependent conductance spectroscopy.

In the third scenario, we flip the spin of $D3$ into spin-down while keeping the other two dots unchanged. This can be experimentally implemented by varying the voltage of a nearby electrostatic gate. The chemical potential of $A2$ is still chosen to be positive: $\varepsilon_{A2} \approx 1.3\Delta_0$, which now gives a same-sign sweet spot as predicted in Fig. 1(f). Indeed, numerical calculations of conductance in Figs. 2(h) and 2(i) confirm that this configuration corresponds to a sign-ordered three-site Kitaev chain. Thereby flipping the spin of the dot orbitals provides an additional knob for eliminating π -phase domain wall.

Protocol for scaling up.—With the findings in the previous sections, we now put forward our protocol for scaling up a sign-ordered Kitaev chain. To this end, we require an experimental setup that can (i) be used to tune two neighboring dots to a sweet spot, for example as discussed in [20–22, 28], and (ii) detect whether the zero-energy degeneracy splits when the energy of the final dot is detuned from zero. In general, this requires that the superconducting leads that proximitize different hybrid regions form a single grounded lead. The two measurements can be realized for example by coupling each normal dot to an individual normal lead, forming a multi-terminal junction, as shown in the device setup in Fig. 3. Alternatively, it is also sufficient to only contact the final dot with a normal lead, as shown in Fig. 2. Further, we expect that gate sensing may also be used to obtain the same effect.

Our protocol allows to build up an effective Kitaev chain iteratively dot by dot.

Step-0: In the beginning of an iteration, we assume that we have already obtained a sign-ordered N -site Kitaev chain ($N \geq 2$) as shown in Fig. 3(a) (for $N = 2$, this corresponds to finding the sweet spot). Our goal is to extend the chain length to $N + 1$ by choosing an appropriate sweet spot for the newly added dot. This can be achieved in two steps.

Step-1: First, we focus on a two-site system formed by the N and $N + 1$ -th quantum dots, which should be decoupled from the rest of the array [see Fig. 3(b)]. This

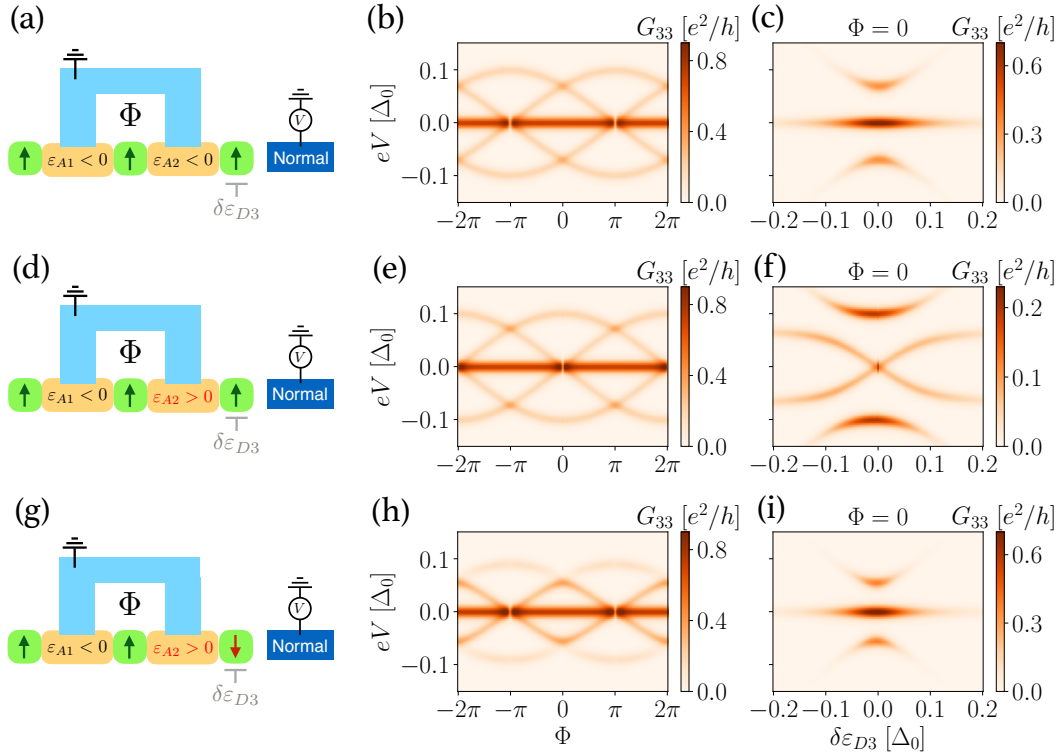


FIG. 2. Left column: Schematics for a three-quantum-dot device with magnetic flux control. Middle column: Conductance spectroscopy ($G_{33} = dI_3/dV_3$) as a function of the magnetic flux. Right column: Conductance spectroscopy as a function of the dot energy detuning. The devices in panels (a) and (g) behave as a sign-ordered three-site Kitaev chain at $\Phi = 0$, while that in panel (d) is subject to a π -phase domain wall.

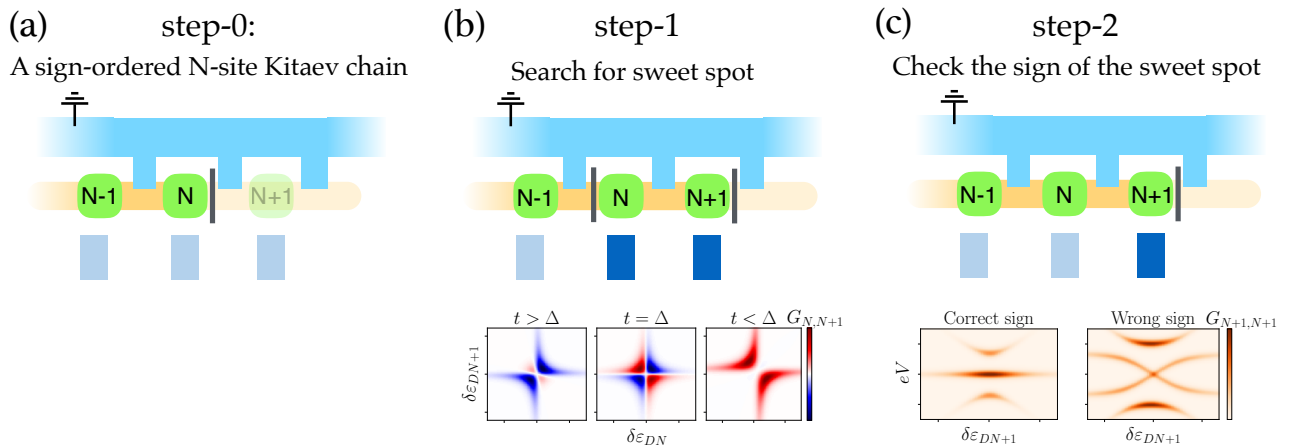


FIG. 3. Protocol for tuning up a long sign-ordered Kitaev chain. (a) Preparation: get ready a sign-ordered N -site Kitaev chain ($N \geq 2$). (b) Step-1: Switch on the coupling between the N and $N+1$ -th dots while decoupling them from the rest of the system. The vertical grey bars denote the tunnel barriers. Find the sweet spot $|t| = |\Delta|$ in the charge stability diagram by fine-tuning the chemical potential of the hybrid region. (c) Step-2: Connect the N -th dot with all the previous $N-1$ dots, and measure the differential conductance in the $N+1$ -th lead versus the detuning energy of the $N+1$ -th dot. If the zero-bias conductance peak remains robust, we thereby obtain a sign-ordered $N+1$ -site Kitaev chain. Otherwise, we should return to step-1 to find a new sweet spot and test it in step-2 until success.

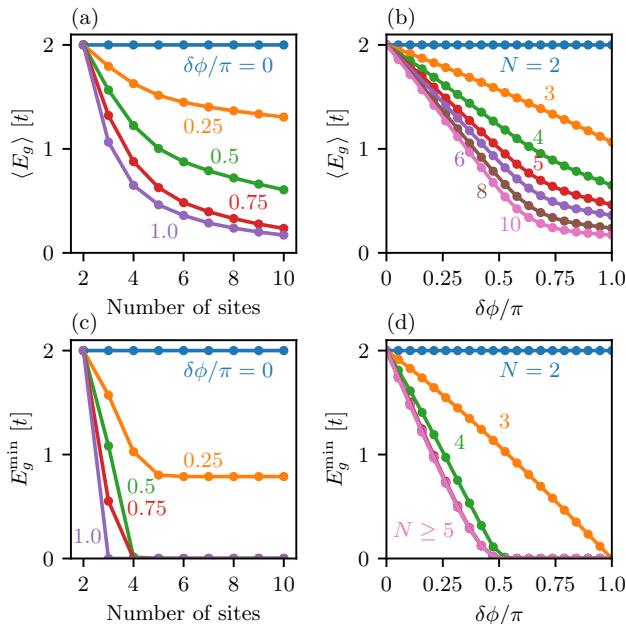


FIG. 4. (a) and (b) Mean of excitation gap of a Kitaev chain versus number of sites and phase fluctuation amplitude. (c) and (d) Minimal excitation gap versus number of sites and phase fluctuation amplitude.

can be achieved by tuning the tunnel barriers, or alternatively by shifting dots from 0 to $N - 1$ away from resonance [35]. Then by varying the chemical potential in the hybrid region, which fine-tunes the ratio of normal and superconducting couplings, a sweet spot ($|t_N| = |\Delta_N|$) can be reached, e.g. signified by a cross in the charge stability diagram [see Fig. 3(b)] [20–22, 27, 28]. However, the sign of the sweet spot remains uncertain so far.

Step-2: In the second step, we form an $N + 1$ -site Kitaev chain by coupling the N and $N + 1$ -th dots to the rest of the chain, e.g. by lowering tunnel barriers or by bringing the $N - 1$ -th dot back to resonance. If the chain is sign-ordered, the zero-energy degeneracy is robust against detuning the on-site energy of dot $N + 1$, otherwise the detuning will lead to a splitting, as shown above. This can be measured, e.g. using conductance spectroscopy on the $N + 1$ -th dot as a function of its detuning energy, as shown in Fig. 3(c). If the degeneracy is robust, we have successfully extended an N -site Kitaev chain to length $N + 1$ and can continue with the next dot. On the other hand, with a wrong sign, the degeneracy will split (as e.g. detected in conductance spectroscopy) and we have to return to step-1 to tune to the other sweet spot or the other dot spin, effectively flipping the relative sign between t and Δ .

Effect of phase fluctuations—We now consider the effect of finite phases beyond 0 and π on the Kitaev chain, i.e. when the complex conjugate symmetry is broken. In a realistic experimental device, this can be caused by

a finite width of the one-dimensional channel, the orbital effect of magnetic field on the quantum dot or ABS wavefunctions, or the applied magnetic field being misaligned from the nanowire axis. After performing an appropriate gauge transformation, an N -site Kitaev chain ($N \geq 3$) can have $N - 2$ independent phase fluctuations i.e. $\Delta_i = |\Delta_i|e^{i\delta\phi_i}$ for $i = 2, 3, \dots, N - 1$ [46]. We emphasize that once the coupling magnitudes are at the sweet spot, i.e. $|t_i| = |\Delta_i|$, phase fluctuations cannot perturb the presence of zero energy, and it mainly affects the size of the excitation gap. Therefore our focus is on how the energy gap scales with the number of sites and the amplitudes of the phase fluctuations. In our model phase fluctuation obeys a uniform distribution of $\delta\phi_i \in [-\delta\phi, \delta\phi]$, and we consider an ensemble of 2000 different phase realizations for each configuration. As shown in Figs. 4(a) and 4(b), the averaged gap size decreases monotonically with both the number of sites and the phase fluctuation amplitude, the latter of which is consistent with the numerical simulations shown in Fig. 2. In addition, Figs. 4(c) and 4(d) show the minimal excitation gap, corresponding to the worst case among the 2000 realizations. Interestingly, a longer chain is more prone to becoming gapless when $\delta\phi > \pi/2$. We hence expect that our protocol remains applicable even for small deviations from one-dimensionality, as the sign of the sweet spot can still be used to minimize the phase difference between neighboring dots.

Summary.—In this work, we discover that the sweet spot mediated by Andreev bound states has a sign uncertainty, which has no effect on two-site chains, but will become crucial for studies of longer quantum dot chains. We further give a concrete protocol for how to scale up an effective Kitaev chain systematically using only electrostatic gates and without flux control. This will greatly simplify the design of experimental devices by eliminating the need for bias flux lines [see Fig. 1(a) and 1(b)]. It avoids the adverse heating issue and also makes the devices much more scalable (quantum dots are ~ 200 nm long while size of bias lines is $\sim 10 \mu\text{m}$), both of which will benefit the eventual implementation of a topological quantum computer. Thus, our work provides physical insight and practical guidance for future experiments aimed at realizing a longer Kitaev chain with topological protection.

Author contributions.—C.-X.L. conceived the project idea and designed the project with input from A.B., S.L.D.t.H. and M.W. C.-X.L. carried out the calculations with input from S.M. and A.M.B. C.-X.L. and M.W. wrote the manuscript with input from all authors. C.-X.L. and M.W. supervised the project.

Acknowledgements.—We are grateful to G. P. Mazur, N. van Loo, F. Zatelli, and L. P. Kouwenhoven for useful discussions. This work was supported by a subsidy for top consortia for knowledge and innovation (TKI toeslag), by the Dutch Organization for Scientific Research (NWO) through OCENW.GROOT.2019.004, and by Microsoft Corporation Station Q.

-
- [1] A Yu Kitaev, “Unpaired Majorana fermions in quantum wires,” *Physics-Uspekhi* **44**, 131 (2001).
- [2] Jason Alicea, “New directions in the pursuit of Majorana fermions in solid state systems,” *Rep. Prog. Phys.* **75**, 076501 (2012).
- [3] Martin Leijnse and Karsten Flensberg, “Introduction to topological superconductivity and Majorana fermions,” *Semicond. Sci. Technol.* **27**, 124003 (2012).
- [4] C.W.J. Beenakker, “Search for Majorana fermions in superconductors,” *Annu. Rev. Condens. Matter Phys.* **4**, 113–136 (2013).
- [5] Tudor D Stanescu and Sumanta Tewari, “Majorana fermions in semiconductor nanowires: fundamentals, modeling, and experiment,” *J. Phys.: Condens. Matter* **25**, 233201 (2013).
- [6] Jian-Hua Jiang and Si Wu, “Non-Abelian topological superconductors from topological semimetals and related systems under the superconducting proximity effect,” *J. Phys.: Condens. Matter* **25**, 055701 (2013).
- [7] Steven R. Elliott and Marcel Franz, “Colloquium: Majorana fermions in nuclear, particle, and solid-state physics,” *Rev. Mod. Phys.* **87**, 137–163 (2015).
- [8] Masatoshi Sato and Satoshi Fujimoto, “Majorana fermions and topology in superconductors,” *J. Phys. Soc. Jpn.* **85**, 072001 (2016).
- [9] Masatoshi Sato and Yoichi Ando, “Topological superconductors: a review,” *Rep. Prog. Phys.* **80**, 076501 (2017).
- [10] Ramón Aguado, “Majorana quasiparticles in condensed matter,” *La Rivista del Nuovo Cimento* **40**, 523–593 (2017).
- [11] R. M. Lutchyn, E. P. A. M. Bakkers, L. P. Kouwenhoven, P. Krogstrup, C. M. Marcus, and Y. Oreg, “Majorana zero modes in superconductor–semiconductor heterostructures,” *Nat. Rev. Mater.* **3**, 52–68 (2018).
- [12] Hao Zhang, Dong E. Liu, Michael Wimmer, and Leo P. Kouwenhoven, “Next steps of quantum transport in Majorana nanowire devices,” *Nat. Commun.* **10**, 5128 (2019).
- [13] Elsa Prada, Pablo San-Jose, Michiel W. A. de Moor, Attila Geresdi, Eduardo J. H. Lee, Jelena Klinovaja, Daniel Loss, Jesper Nygård, Ramón Aguado, and Leo P. Kouwenhoven, “From andreev to majorana bound states in hybrid superconductor–semiconductor nanowires,” *Nature Reviews Physics* **2**, 575–594 (2020).
- [14] S. M. Frolov, M. J. Manfra, and J. D. Sau, “Topological superconductivity in hybrid devices,” *Nature Physics* **16**, 718–724 (2020).
- [15] Karsten Flensberg, Felix von Oppen, and Ady Stern, “Engineered platforms for topological superconductivity and majorana zero modes,” *Nature Reviews Materials* **6**, 944–958 (2021).
- [16] Chetan Nayak, Steven H. Simon, Ady Stern, Michael Freedman, and Sankar Das Sarma, “Non-Abelian anyons and topological quantum computation,” *Rev. Mod. Phys.* **80**, 1083–1159 (2008).
- [17] Sankar Das Sarma, Michael Freedman, and Chetan Nayak, “Majorana zero modes and topological quantum computation,” *Npj Quantum Information* **1**, 15001 EP – (2015).
- [18] Jay D. Sau and S. Das Sarma, “Realizing a robust practical Majorana chain in a quantum-dot-superconductor linear array,” *Nat. Commun.* **3**, 964 (2012).
- [19] Martin Leijnse and Karsten Flensberg, “Parity qubits and poor man’s Majorana bound states in double quantum dots,” *Phys. Rev. B* **86**, 134528 (2012).
- [20] Tom Dvir, Guanzhong Wang, Nick van Loo, Chun-Xiao Liu, Grzegorz P. Mazur, Alberto Bordin, Sebastiaan L. D. ten Haaf, Ji-Yin Wang, David van Driel, Francesco Zatelli, Xiang Li, Filip K. Malinowski, Sasa Gazibegovic, Ghada Badawy, Erik P. A. M. Bakkers, Michael Wimmer, and Leo P. Kouwenhoven, “Realization of a minimal kitaev chain in coupled quantum dots,” *Nature* **614**, 445–450 (2023).
- [21] Sebastiaan L. D. ten Haaf, Qingzhen Wang, A. Mert Bozkurt, Chun-Xiao Liu, Ivan Kulesh, Philip Kim, Di Xiao, Candice Thomas, Michael J. Manfra, Tom Dvir, Michael Wimmer, and Srijit Goswami, “A two-site kitaev chain in a two-dimensional electron gas,” *Nature* **630**, 329–334 (2024).
- [22] Francesco Zatelli, David van Driel, Di Xu, Guanzhong Wang, Chun-Xiao Liu, Alberto Bordin, Bart Roovers, Grzegorz P. Mazur, Nick van Loo, Jan Cornelis Wolff, *et al.*, “Robust poor man’s majorana zero modes using yu-shiba-rusinov states,” *arXiv:2311.03193* (2023).
- [23] Chun-Xiao Liu, Guanzhong Wang, Tom Dvir, and Michael Wimmer, “Tunable superconducting coupling of quantum dots via andreev bound states in semiconductor-superconductor nanowires,” *Phys. Rev. Lett.* **129**, 267701 (2022).
- [24] Alberto Bordin, Guanzhong Wang, Chun-Xiao Liu, Sebastiaan L. D. ten Haaf, Nick van Loo, Grzegorz P. Mazur, Di Xu, David van Driel, Francesco Zatelli, Sasa Gazibegovic, Ghada Badawy, Erik P. A. M. Bakkers, Michael Wimmer, Leo P. Kouwenhoven, and Tom Dvir, “Tunable crossed andreev reflection and elastic cotunneling in hybrid nanowires,” *Phys. Rev. X* **13**, 031031 (2023).
- [25] Guanzhong Wang, Tom Dvir, Grzegorz P. Mazur, Chun-Xiao Liu, Nick van Loo, Sebastiaan L. D. ten Haaf, Alberto Bordin, Sasa Gazibegovic, Ghada Badawy, Erik P. A. M. Bakkers, Michael Wimmer, and Leo P. Kouwenhoven, “Singlet and triplet cooper pair splitting in hybrid superconducting nanowires,” *Nature* **612**, 448–453 (2022).
- [26] Qingzhen Wang, Sebastiaan L. D. ten Haaf, Ivan Kulesh, Di Xiao, Candice Thomas, Michael J. Manfra, and Srijit Goswami, “Triplet correlations in cooper pair splitters realized in a two-dimensional electron gas,” *Nat. Commun.* **14**, 4876 (2023).
- [27] Athanasios Tsintzis, Rubén Seoane Souto, and Martin Leijnse, “Creating and detecting poor man’s majorana bound states in interacting quantum dots,” *Phys. Rev. B* **106**, L201404 (2022).
- [28] Chun-Xiao Liu, A Mert Bozkurt, Francesco Zatelli, Sebastiaan LD ten Haaf, Tom Dvir, and Michael Wimmer, “Enhancing the excitation gap of a quantum-dot-based kitaev chain,” *arXiv:2310.09106* (2023).
- [29] Rubén Seoane Souto, Athanasios Tsintzis, Martin Leijnse, and Jeroen Danon, “Probing majorana localization in minimal kitaev chains through a quantum dot,” *Phys. Rev. Res.* **5**, 043182 (2023).
- [30] Sebastian Miles, David van Driel, Michael Wimmer, and

- Chun-Xiao Liu, “Kitaev chain in an alternating quantum dot-andreev bound state array,” [arXiv:2309.15777 \(2023\)](#).
- [31] Juan Daniel Torres Luna, A Mert Bozkurt, Michael Wimmer, and Chun-Xiao Liu, “Flux-tunable kitaev chain in a quantum dot array,” [arXiv:2402.07575 \(2024\)](#).
- [32] William Samuelson, Viktor Svensson, and Martin Leijnse, “Minimal quantum dot based kitaev chain with only local superconducting proximity effect,” *Phys. Rev. B* **109**, 035415 (2024).
- [33] Rubén Seoane Souto and Ramón Aguado, “Subgap states in semiconductor-superconductor devices for quantum technologies: Andreev qubits and minimal majorana chains,” [arXiv:2404.06592 \(2024\)](#).
- [34] Alberto Bordin, Xiang Li, David van Driel, Jan Cornelis Wolff, Qingzhen Wang, Sebastiaan L. D. ten Haaf, Guanzhong Wang, Nick van Loo, Leo P. Kouwenhoven, and Tom Dvir, “Crossed andreev reflection and elastic cotunneling in three quantum dots coupled by superconductors,” *Phys. Rev. Lett.* **132**, 056602 (2024).
- [35] Alberto Bordin, Chun-Xiao Liu, Tom Dvir, Francesco Zatelli, Sebastiaan LD ten Haaf, David van Driel, Guanzhong Wang, Nick van Loo, Thomas van Caekenberghe, Jan Cornelis Wolff, *et al.*, “Signatures of majorana protection in a three-site kitaev chain,” [arXiv:2402.19382 \(2024\)](#).
- [36] Motohiko Ezawa, “Even-odd effect on robustness of majorana edge states in short kitaev chains,” *Phys. Rev. B* **109**, L161404 (2024).
- [37] Sumanta Tewari and Jay D. Sau, “Topological invariants for spin-orbit coupled superconductor nanowires,” *Phys. Rev. Lett.* **109**, 150408 (2012).
- [38] Matthias Scheid, İnanç Adagideli, Junsaku Nitta, and Klaus Richter, “Anisotropic universal conductance fluctuations in disordered quantum wires with rashba and dresselhaus spin-orbit interaction and an applied in-plane magnetic field,” *Semiconductor Science and Technology*, **24**, 064005 (2009).
- [39] M. Diez, J. P. Dahlhaus, M. Wimmer, and C. W. J. Beenakker, “Andreev reflection from a topological superconductor with chiral symmetry,” *Phys. Rev. B* **86**, 094501 (2012).
- [40] Zhi-Hai Liu, Chuanchang Zeng, and H. Q. Xu, “Coupling of quantum-dot states via elastic-cotunneling and crossed andreev reflection in a minimal kitaev chain,” [arXiv:2403.08636 \(2024\)](#).
- [41] A Mert Bozkurt, Sebastian Miles, Sebastiaan LD ten Haaf, Chun-Xiao Liu, Fabian Hassler, and Michael Wimmer, “Interaction-induced strong zero modes in short quantum dot chains with time-reversal symmetry,” [arXiv:2405.14940 \(2024\)](#).
- [42] David van Driel, Rouven Koch, Vincent PM Sietses, Sebastiaan LD ten Haaf, Chun-Xiao Liu, Francesco Zatelli, Bart Roovers, Alberto Bordin, Nick van Loo, Guanzhong Wang, *et al.*, “Cross-platform autonomous control of minimal kitaev chains,” [arXiv:2405.04596 \(2024\)](#).
- [43] Fernando Domínguez and Alfredo Levy Yeyati, “Quantum interference in a cooper pair splitter: The three sites model,” *Physica E: Low-dimensional Systems and Nanostructures* **75**, 322–329 (2016).
- [44] Tudor D. Stanescu, Jay D. Sau, Roman M. Lutchyn, and S. Das Sarma, “Proximity effect at the superconductor-topological insulator interface,” *Phys. Rev. B* **81**, 241310 (2010).
- [45] Andrey E. Antipov, Arno Bargerbos, Georg W. Winkler, Bela Bauer, Enrico Rossi, and Roman M. Lutchyn, “Effects of gate-induced electric fields on semiconductor Majorana nanowires,” *Phys. Rev. X* **8**, 031041 (2018).
- [46] See supplemental materials for 1. Gauge transformation of Kitaev chain 2.Effect of finite Zeeman energy in the Andreev bound states 3.hybridization of Majorana modes at π phase.
- [47] C. W. J. Beenakker, “Theory of coulomb-blockade oscillations in the conductance of a quantum dot,” *Phys. Rev. B* **44**, 1646–1656 (1991).
- [48] Henrik Bruus and Karsten Flensberg, *Many-body quantum theory in condensed matter physics: an introduction* (OUP Oxford, 2004).

Supplemental Materials for “Protocol for scaling up a sign-ordered Kitaev chain without magnetic flux control”

I. GAUGE TRANSFORMATION ON KITAEV CHAIN

The Hamiltonian of an N -site spinless Kitaev chain is given by

$$H_K = \sum_{n=1}^N \varepsilon_n f_n^\dagger f_n + \sum_{n=1}^{N-1} (t_n e^{i\alpha_n} f_{n+1}^\dagger f_n + \Delta_n e^{i\beta_n} f_{n+1}^\dagger f_n^\dagger + h.c.). \quad (\text{S-1})$$

Here $\varepsilon_n, t_n, \Delta_n > 0$ and $0 \leq \alpha_n, \beta_n < 2\pi$ without loss of generality. We now perform a gauge transformation on the spinless fermion operators as below

$$\begin{aligned}\tilde{f}_n &= f_n e^{i\theta_n}, & \tilde{f}_n^\dagger &= f_n^\dagger e^{-i\theta_n}, \\ \theta_1 &= -(\alpha_1 + \beta_1)/2, \\ \theta_2 &= (\alpha_1 - \beta_1)/2, \\ \theta_{n+1} &= \theta_n + \alpha_n \quad (n \geq 1),\end{aligned}\tag{S-2}$$

such that we now obtain the most general form of the Kitaev chain Hamiltonian

$$H_K = \sum_{n=1}^N \varepsilon_n \tilde{f}_n^\dagger \tilde{f}_n + \sum_{n=1}^{N-1} (t_n \tilde{f}_{n+1}^\dagger \tilde{f}_n + \Delta_n e^{i\phi_n} \tilde{f}_{n+1}^\dagger \tilde{f}_n^\dagger + h.c.),\tag{S-3}$$

where $\phi_1 = 0$ and

$$\phi_n = \phi_{n-1} + (\beta_n - \beta_{n-1}) + (\alpha_n + \alpha_{n-1})\tag{S-4}$$

for $n \geq 2$. This indicates that phase plays no role in a minimal two-site chain and becomes important only when $N \geq 3$.

II. FINITE ZEEMAN SPIN SPLITTING IN THE ANDREEV BOUND STATES

In this section, we consider a weak Zeeman spin splitting in the Andreev bound state and show that the two opposite-sign sweet spots still exists. The only difference compared to zero-Zeeman scenario is that now the gap sizes at the two sweet spots become different. The only modification we make in the Hamiltonian of Eq. (3) is

$$H_{A,i} = \sum_{\sigma=\uparrow,\downarrow} (\varepsilon_{Ai} + \sigma E_Z) n_{Ai\sigma} + (\Delta_i c_{Ai\uparrow}^\dagger c_{Ai\downarrow} + h.c.).\tag{S-5}$$

with $E_Z \ll \Delta$. Using the second-order perturbation theory, the ECT and CAR between orbitals of same spins $H_{\text{eff}}(E_Z) = t_{\uparrow\uparrow} c_{R\uparrow}^\dagger c_{L\uparrow} + \Delta_{\uparrow\uparrow} c_{R\uparrow}^\dagger c_{L\uparrow}^\dagger + h.c.$ are

$$\begin{aligned}t_{\uparrow\uparrow}(E_Z) &= -t_{\text{sc},1} t'_{\text{sc},1} \left(\frac{u^2}{E_A + E_Z} - \frac{v^2}{E_A - E_Z} \right) + t_{\text{sf},1} t'_{\text{sf},1} \left(\frac{u^2}{E_A - E_Z} - \frac{v^2}{E_A + E_Z} \right) \\ \Delta_{\uparrow\uparrow}(E_Z) &= (t_{\text{sc},1} t'_{\text{sf},1} + t_{\text{sf},1} t'_{\text{sc},1}) \left(\frac{uv}{E_A + E_Z} + \frac{uv}{E_A - E_Z} \right).\end{aligned}\tag{S-6}$$

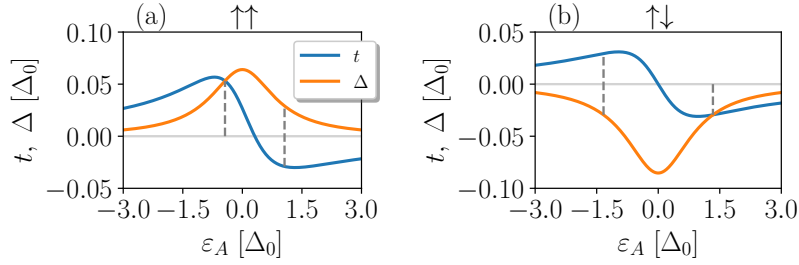
Similarly, for the opposite-spin orbitals, we have

$$\begin{aligned}t_{\uparrow\downarrow}(E_Z) &= -t_{1\text{sc}} t'_{1\text{sf}} \left(\frac{u^2}{E_A + E_Z} - \frac{v^2}{E_A - E_Z} \right) - t_{1\text{sf}} t'_{1\text{sc}} \left(\frac{u^2}{E_A - E_Z} - \frac{v^2}{E_A + E_Z} \right), \\ \Delta_{\uparrow\downarrow}(E_Z) &= (t_{1\text{sf}} t'_{1\text{sf}} - t_{1\text{sc}} t'_{1\text{sc}}) \left(\frac{uv}{E_A + E_Z} + \frac{uv}{E_A - E_Z} \right).\end{aligned}\tag{S-7}$$

The profiles of ECT and CAR for $E_Z/\Delta_0 = 0.25$ are shown in Fig. S1. For the same-spin channel, the two sweet spots are no longer symmetric about ε_A , they appear at $\varepsilon_A^* \approx -0.437\Delta_0$ and $\varepsilon_A^* \approx 1.062\Delta_0$. For the opposite-spin channel, we still have $\varepsilon_A^* = \pm 4\Delta_0/3$. We thus conclude that the findings of two sweet spots with opposite signs presented in the main text are robust against a weak Zeeman spin splitting in the ABS. The presence of such a weak Zeeman field only modifies some details of the sweet spot, e.g., sweet-spot values of ε_A and strength of $|t|$.

III. SPLITTING OF ZERO MODES AT π PHASE

Here we provide a theoretical understanding for why the zero energy at π phase gets split against detuning of the outermost dot. Without loss of generality, we consider the spinless model for a three-site Kitaev chain. The



Supplementary Figure S1. CAR and ECT profiles in same- and opposite-spin channels in the presence of a weak Zeeman spin splitting ($E_Z/\Delta_0 = 0.25$) in ABS. There still exist two sweet spots with opposite signs.

Bogoliubov-de Gennes Hamiltonian is

$$H_3 = \begin{pmatrix} \varepsilon_1 & t_1 & 0 & 0 & \Delta_1 & 0 \\ t_1 & \varepsilon_2 & t_2 & -\Delta_1 & 0 & \Delta_2 \\ 0 & t_2 & \varepsilon_3 & 0 & -\Delta_2 & 0 \\ 0 & -\Delta_1 & 0 & -\varepsilon_1 & -t_1 & 0 \\ \Delta_1 & 0 & -\Delta_2 & -t_1 & -\varepsilon_2 & -t_2 \\ 0 & \Delta_2 & 0 & 0 & -t_2 & -\varepsilon_3 \end{pmatrix} = \begin{pmatrix} 0 & t_1 & 0 & 0 & t_1 & 0 \\ t_1 & 0 & t_2 & -t_1 & 0 & -t_2 \\ 0 & t_2 & 0 & 0 & t_2 & 0 \\ 0 & -t_1 & 0 & 0 & -t_1 & 0 \\ t_1 & 0 & t_2 & -t_1 & 0 & -t_2 \\ 0 & -t_2 & 0 & 0 & -t_2 & 0 \end{pmatrix} \quad (\text{S-8})$$

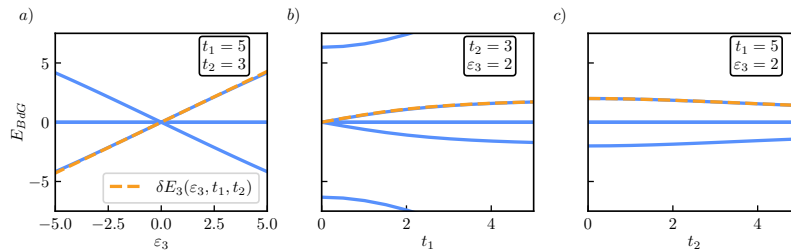
under the basis of $(f_1, f_2, f_3, f_1^\dagger, f_2^\dagger, f_3^\dagger)$. Here we choose $\varepsilon_1 = \varepsilon_2 = \varepsilon_3 = 0, t_1 = \Delta_1$, and $t_2 = -\Delta_2$ at π phase. There exist four Majorana zero modes at this point, with their wavefunctions being

$$\begin{aligned} \psi_1 &= (1, 0, 0, 1, 0, 0)^T/\sqrt{2}, \\ \psi_2 &= (0, -i, 0, 0, i, 0)^T/\sqrt{2}, \\ \psi_3 &= (0, 0, 1, 0, 0, 1)^T/\sqrt{2}, \\ \psi_4 &= (it_2, 0, -it_1, -it_2, 0, it_1)^T/\sqrt{2(t_1^2 + t_2^2)}. \end{aligned} \quad (\text{S-9})$$

Note that the first three Majoranas are localized at dots-1,2,3, while the fourth one is delocalized at the dots-1 and -3. When the energy level of the third dot is detuned from resonance, the perturbation Hamiltonian is $H' = \text{diag}(0, 0, \delta\varepsilon_3, 0, 0, -\delta\varepsilon_3)$, coupling the third and fourth Majorana modes. The resulting energy splitting is therefore

$$\delta E \approx |\langle \psi_3 | H' | \psi_4 \rangle| = \frac{t_1}{\sqrt{t_1^2 + t_2^2}} \times \delta\varepsilon_3. \quad (\text{S-10})$$

That is, to the leading order, the energy is split linearly, with the coefficient determined by the parameters t_1 and t_2 . To verify our analytic results, we numerically calculate the energy spectra of a three-site Kitaev chain model as a function of ε_3, t_1, t_2 , as shown in Fig. S2. The numerical results are in excellent agreement with the analytic ones.



Supplementary Figure S2. Energy spectra of Bogoliubov-de Gennes Hamiltonian in the vicinity of the sweet spot with $\phi = \pi$ as a function of ε_3, t_1, t_2 . The numerically calculated splitting of the zero energy (solid blue lines) is in excellent agreement with the analytic results (dashed orange lines).